

PING-Mapper: open-source software for automated benthic imaging and mapping using recreation-grade sonar

This is a Preprint and has not been peer reviewed.

Authors:

Cameron S. Bodine, *csb67@nau.edu*

School of Informatics, Computing, and Cyber Systems, Northern Arizona University, Flagstaff, Arizona, USA.

Daniel Buscombe

School of Informatics, Computing, and Cyber Systems, Northern Arizona University, Flagstaff, Arizona, USA.

School of Earth and Sustainability, Northern Arizona University, Flagstaff, Arizona, USA.

Rebecca J. Best

School of Earth and Sustainability, Northern Arizona University, Flagstaff, Arizona, USA.

Jennylyn A. Rednert

Arizona Natural Heritage Program, Arizona Game and Fish Department, Phoenix, Arizona, USA..

Adam J. Kaeser

U.S. Fish and Wildlife Service, Panama City Fish and Wildlife Conservation Office, Panama City, Florida, USA.

Key Points:

- We developed an open-source software for exporting benthic datasets and georeferenced imagery from Humminbird side scan sonar systems.
- Software provides automated and reproducible approach to processing sonar data with minimal interaction from the user.
- Three case studies are presented to highlight use cases of processed benthic datasets.

June 13, 2022

Associated software, PING-Mapper: <https://github.com/CameronBodine/PINGMapper>

PING-Mapper: open-source software for automated benthic imaging and mapping using recreation-grade sonar

C. S. Bodine¹, D. Buscombe^{1,2}, R. J. Best², J. A. Redner³, and A. J. Kaeser⁴

¹School of Informatics, Computing, and Cyber Systems, Northern Arizona University, Flagstaff, Arizona, USA.

²School of Earth and Sustainability, Northern Arizona University, Flagstaff, Arizona, USA.

³Arizona Natural Heritage Program, Arizona Game and Fish Department, Phoenix, Arizona, USA.

⁴U.S. Fish and Wildlife Service, Panama City Fish and Wildlife Conservation Office, Panama City, Florida, USA.

June 13, 2022

Abstract

The characterization of benthic habitats is essential for aquatic ecosystem science and management, but is frequently limited by waterbody visibility and depth. Recreation-grade side scan sonar systems are increasingly used to aid scientific inquiries in shallow water due to their relative low-cost, ease of operation, low-weight, and ease of mounting on a variety of vessels. However, existing procedures and software for post-processing these data are either limited, closed source, or fail on data from new sonar models; limiting development of reproducible workflows. Here we present PING-Mapper, an open source and freely available side scan sonar post-processing toolset for processing and mapping sonar recordings from popular Humminbird instruments. The modular software automatically: 1) decodes sonar recordings from any Humminbird system; 2) exports ping attributes from every sonar channel; 3) uses sonar sensor depth or automated depth detection for water column removal; and 4) exports sonogram tiles and georectified mosaics. Sonar channels are processed in parallel for quick decoding and metadata extraction. Workflows for major processing workflows including georectification and image export scale with computing resources. The software has been extensively tested using data from several river distributaries of varying character and distribution of depths, but could also be used in estuarine and lacustrine environments. Usage of PING-Mapper is illustrated in three case studies focused on mapping large woody debris, bathymetric mapping, and visual interpretation and mapping of substrates for select reaches of the Pearl and Pascagoula river systems in Mississippi.

Keywords– Acoustic remote sensing, Sidescan sonar, Benthic habitat

Plain Language Summary

Side scan sonar instruments provide a way to survey and visualize the bottom of rivers, lakes, or oceans. Since the early 2000s, companies catering predominantly to anglers have manufactured recreation-grade side scan sonar systems to aid fishermen in locating fish and identifying potential hazards. Scientists seeking to understand and manage aquatic habitats soon found use in these systems to create grayscale images of water bottoms because they are inexpensive, are easy to operate, and require minimal mounting equipment on the boat. Software has been created by companies to process these data, but the underlying processing workflow and computer code are not publicly available, which makes it difficult to reproduce and compare results among multiple scientists and studies. Other publicly available approaches and software are either outdated, not maintained, or not free. That is why we made PING-Mapper. This software is built using a

programming language called Python, an increasingly popular language used by many scientists. All the code of PING-Mapper is made freely available. We designed the software to work on any computer with minimal hardware specifications, to export the desired datasets as quickly as possible. We demonstrate the use of the exported datasets with three case studies focused on common scientific usages, locating and mapping targets (specifically large trees and branches), creating depth maps, and visually discerning the distributions of common substrates such as sand and cobble.

1 Introduction

Our understanding of the Earth’s surface and atmosphere has benefited from large investments in air and space-borne observation systems, such as NASA’s Earth Observation System (EOS) (Murphy, 2021), providing unparalleled ability to model the climate (Yang et al., 2013), track landcover changes (Weiers et al., 2004; Bock et al., 2005), or map species-specific habitat availability (Kerr & Ostrovsky, 2003). In comparison, the spatial and temporal extent of our knowledge of aquatic environments, particularly shallow freshwater habitats, remains limited. This leaves scientists and managers with less information to address threats to species that depend on freshwater systems (Barnosky et al., 2011; Tickner et al., 2020). Shallow waterbodies are ubiquitous; 85% of the world’s 3.5M rivers have an average depth of 1m (Andreadis et al., 2013), and the average depth of the world’s 27M lakes is 41.8m, with 99% of lakes less than 10m in depth (Cael et al., 2017). Shallow water, particularly small waterbodies (Biggs et al., 2017), are disproportionately important for aquatic biodiversity including macrophytes (Fu et al., 2014), bacteria, diatoms and chironomids (Zhao et al., 2019); macrobenthos (Musale & Desai, 2010); plankton (Longhurst, 2007); pelagic fish (Smith & Brown, 2002); and assemblages of marine meiofauna, macrofauna, and megafauna (Danovaro et al., 2010).

Techniques available for mapping in-stream habitat depend on the species of interest, type of system, parameters of interest, and spatial scale (Myrsvold & Dervo, 2020), however traditional techniques for collecting these parameters are limited in space and time. Side scan sonar (SSS) is an effective technology for efficiently collecting large swaths of benthic imagery (Chesterman et al., 1958; Klein & Edgerton, 1968; Singh et al., 2000; Brown et al., 2011). Sonar images are geographically rectified (i.e., georectified), converting time and slant-range distance data into a regular Cartesian grid positioned accurately in space using geographic positioning system (GPS) coordinates. Survey-grade systems popular for imaging marine ecosystems are relatively expensive and require substantial technical expertise. It is also more difficult and dangerous to operate hydrographic survey vessels in shallow water. Recreation, or consumer-grade sonar systems (e.g., Humminbird, Lowrance, and Garmin) offer an alternative and are increasingly popular for scientific research (Kaeser & Litts, 2010; Schmidt et al., 2020; Scholl et al., 2021). These systems are comparatively low-cost, portable, and easy to operate and deploy; require minimal power and experience; and can be launched from small watercraft. However, extracting and processing data from these systems remains a major challenge. Leveraging the transformative potential of these systems for scientific research thus requires free and open-source software implementations of scientifically defensible processing workflows that have been tested on a variety of data.

The first method to extract data from Humminbird Side Imaging systems to map shallow water habitat features was a sonar screen snapshot approach (Kaeser & Litts, 2008, 2010). In this method, concurrent overlapping snapshots are captured at regular intervals via live feed imagery on the control head screen. Snapshots can be inadvertently missed, leaving gaps in resulting sonar mosaics. Snapshot image resolution is determined by the control head’s screen size, necessitating larger and more expensive systems. After data collection, tools developed by the authors require time-consuming manual post-processing steps to generate georectified mosaics, limiting batch processing options. The tools are written in Visual Basic for Applications (VBA) and run in potentially cost-prohibitive

87 ESRI ArcGIS software; however, current ArcGIS versions no longer support VBA, ef-
88 fectively rendering this approach obsolete.

89 Many of the limitations of the snapshot approach can be overcome by recording
90 sonar intensity and metadata directly to file, but format and structure are not provided
91 by the manufacturer. Currently, options for processing these files are limited. Decod-
92 ing recordings from early Humminbird models was first demonstrated with PyHum (Buscombe
93 et al., 2016; Buscombe, 2017); an open-source Python toolbox for decoding sonar record-
94 ings, exporting ping metadata (e.g., vessel position, heading, and speed), applying sonar
95 intensity corrections, classifying bed textures, and exporting georectified imagery. The
96 software is limited in application because it only works for older Humminbird models,
97 is difficult to install due to underlying dependencies, and has poor computational effi-
98 ciency. Alternatives to this toolbox have additional limitations. For example, HumViewer
99 (Johansen, 2013) permits users to view the recording but offers limited export function-
100 ality. HumConverter (Parnum et al., 2017) is a free software for decoding sonar record-
101 ings but requires MATLAB (> 1,000 USD) to work with file exports. Low-cost (< 500
102 USD) commercial software such as SonarTRX (Leraand Engineering Inc., 2022) and Reef-
103 Master (ReefMaster Software Ltd., 2021) offer interfaces and tools for viewing, correct-
104 ing, and exporting sonar data. However, source-code for these programs are not housed
105 on public-repositories, limiting opportunities for collaboration, scientific applications re-
106 quiring reproducibility, and modifications or extensions to functionality.

107 This article describes PING-Mapper, a new modular processing engine written in
108 Python 3 that is open-source and free to use. It is similar in scope to PyHum, but works
109 with data from all Humminbird models, is easier to install and maintain, and is more
110 computationally efficient. We have also significantly improved the algorithms for depth
111 detection, and image rectification, and have tested on a larger variety of environmental
112 conditions. The software provides many advantages to the software and methodologies
113 referenced here including: 1) decoding any Humminbird sonar recording, regardless of
114 model (at the time of writing, there are 14 Humminbird side imaging models available);
115 2) batch processing of sonar recordings; 3) export of ping metadata to comma separated
116 value or CSV format files; 4) export of non-rectified imagery; 5) export of georectified
117 imagery; and is 6) publicly hosted in a repository, ensuring workflow transparency, and
118 inviting contributions from the community.

119 2 Implementation

120 The following sections describe PING-Mapper’s processing workflow (Figure 1) for
121 decoding and exporting benthic datasets from Humminbird SSS systems.

122 2.1 Decode Humminbird Files

123 Sonar recording files from a Humminbird sonar instrument are written in a prop-
124 rietary format of ASCII-encoded hexadecimal values. Each sonar scan creates a single
125 DAT file. The DAT file stores metadata when a recording is initialized, including the
126 selected water type (of which there are three; fresh, shallow saltwater, deep saltwater),
127 the Unix time (epoch) in seconds, Easting and Northing in World Geodetic System 1984
128 (WGS 84) World Mercator coordinate reference system, name of the recording, number
129 of pings, initial range setting (i.e., number of ping returns), and length of the record-
130 ing in milliseconds.

131 Along with the DAT file, each active sonar channel, or beam, has an associated SON
132 and IDX file. The SON file stores the pings while the IDX file stores the byte index (the
133 location in the file of the start of each ping) and time elapsed of each ping in the SON
134 file. A ping has two components: 1) ping attributes (termed here as ping header, or sim-

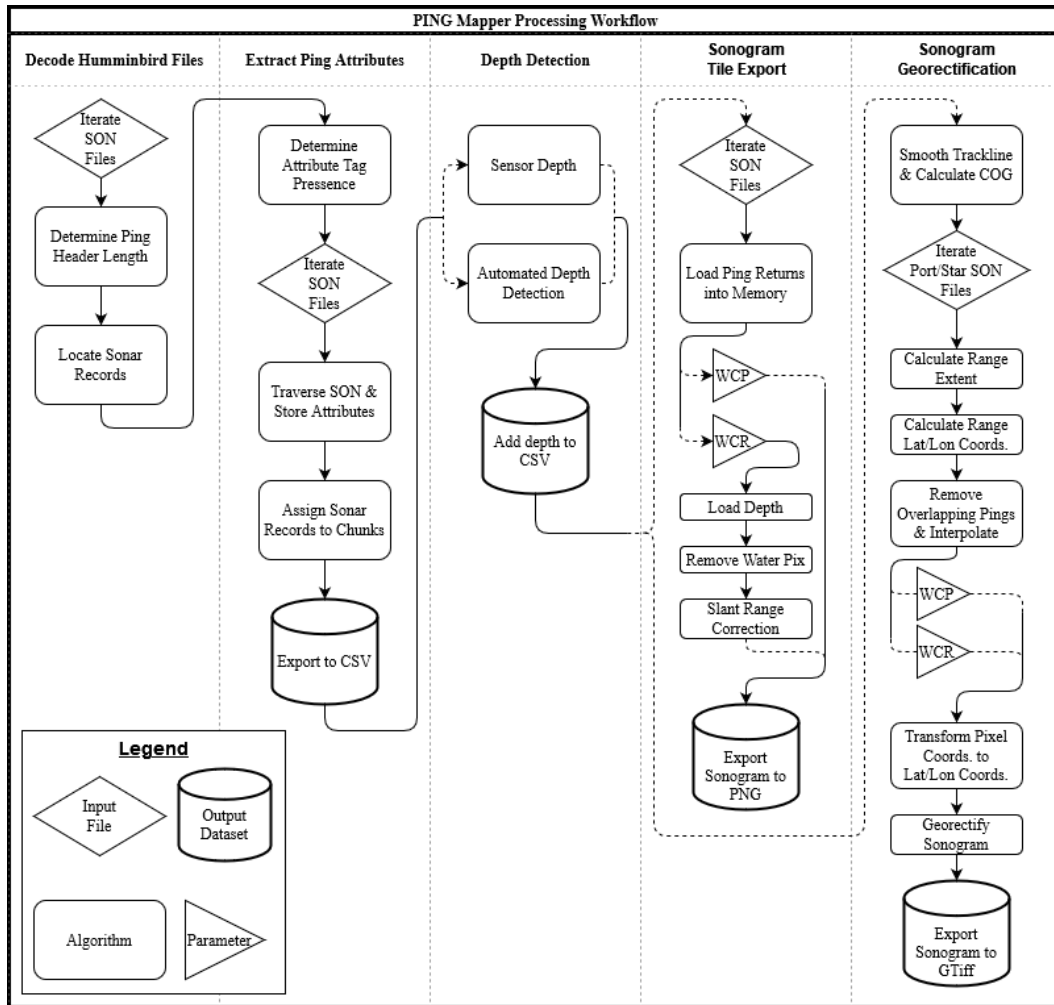


Figure 1. Overview of PING-Mapper processing workflow as described in Section 2. Acronyms are defined as: SON (Humminbird sonar file); CSV (comma-separated values file); WCP (water column present); WCR (water column removed); PNG (portable network graphics); COG (course over ground, i.e., heading); Lat (latitude); Lon (longitude); and GTiff (geospatial tag image file format).

ply header); and 2) ping returns, or acoustic backscatter intensity values, stored in 8-bit [0-255] encoding (Buscombe, 2017).

The number of bytes in a ping vary in two ways. First, the length of the header is dependent on the Humminbird model, with each model storing a varying number of ping attributes (see Supporting Information Table 1). Regardless of the header contents, each starts and ends with the same values, allowing PING-Mapper to automatically determine header length. Second, the ping length (in milliseconds) varies with the number of returns following the header, determined by the range setting at the time of the survey, which in turn dictates the sonar pulse length (Buscombe, 2017). The last attribute in the header indicates the number of returns that follow. The next ping immediately follows the last return of the previous ping, and so on. The IDX file allows quick navigation to the beginning of each sonar record, but these files can become corrupt due to, for example, power failure during the survey. If the IDX file is corrupt or missing, PING-Mapper locates pings based on the header length and number of returns.

2.2 Extract Ping Attributes

For each ping in a SON file, the header stores a series of attributes relating to that ping's returns. Each attribute is tagged with a unique identifier, or name, followed by the attribute's value. All sonar models use consistent naming of a given attribute, but may have additional unused attribute slots. Once pings are located, PING-Mapper decodes each header and exports the attributes to a CSV for each sonar beam. Attributes with valid data contain positional information, time elapsed, depth at nadir, heading, and speed. A list of all attributes and their location based on sonar model is provided in Table 1. These data are used in subsequent georectification procedures, which convert the raw data into a regular spatial grid that can be viewed as a map (see section 2.5).

2.3 Depth Detection

Water depth is a fundamental variable governing river hydraulics, morphologies, sediments, and habitats and is also used to make the necessary geometric corrections to the sonar imagery to recreate continuous planform imagery of the bottom (see sections 2.4-2.5). SSS systems are equipped with down-facing sonar beam(s) that imprecisely estimate the depth at nadir for each sonar record. These data are stored in the SON files for each ping. The estimates are often error-prone due to various mechanical and environmental factors (Yan et al., 2021). Therefore, options to smooth noisy estimates and uniformly adjust the depth to account for sonar transducer offset are provided.

2.4 Sonogram Tile Export

Once ping attributes have been extracted, non-rectified sonar imagery of ping returns, or sonograms, are optionally exported to tiles. PING-Mapper loads ping returns into memory in batches based on chunk size (see Section 2.6). Sonograms can be exported with the water column present (WCP) or water column removed (WCR). WCP images show the water column at nadir, making them suitable for applications of locating and counting fish (Flowers & Hightower, 2013) as well as measuring height of submerged vegetation (Sánchez-Carnero et al., 2012). WCP images require no additional post-processing and can be directly exported to standard image formats. Alternatively, WCR images are most suitable for accurate spatial positioning of the bed as presence of the water column introduces geometric distortions which affect of the bed pixels in the near-field (Cobra et al., 1992), necessitating additional post-processing to generate these sonograms.

A two-step geometric correction to the sonogram is required to remove the water column pixels then relocate the bed pixels horizontally across the track, known as slant

183 range correction (Cobra et al., 1992). The sonar system cannot measure depth across
 184 track, preventing precise calculation of across track distance, or range, to each pixel. There-
 185 fore, a naïve assumption that the bed is flat across the track allows the range to be ap-
 186 proximated using the slant range and depth at nadir. This flat-bed assumption applies
 187 only to the useful portion of riverbed scanned, which is approximately 10-20 times the
 188 water depth as a rule-of-thumb. The flat-bed assumption is calculated piecewise across
 189 the width of the waterbody and bed pixels are redistributed across the track. Gaps in
 190 the data are then filled using a one-dimensional piecewise linear interpolation method.
 191 Non-rectified SRC sonogram tiles can then be exported to standard image formats.

192 2.5 Sonogram Georectification

193 Recreation-grade sonar systems often have an autonomous internal GPS receiver
 194 in the sonar control head. Ports are available to add an external GPS that might have
 195 better positional accuracy. Each sonar record has a single geographic coordinate and the
 196 heading from the GPS. These data are used to warp the sonogram to the vessel track
 197 and geographically locate each pixel, termed here georectification.

198 In a typical side scan survey, the vessel is constantly moving to image the bed. How-
 199 ever, the GPS refresh rate is typically slower than the ping rate, resulting in multiple
 200 sonar records sharing identical coordinates despite the constant movement of the ves-
 201 sel. PING-Mapper performs several corrections to recalculate the coordinates for each
 202 sonar record along the track. First, ping coordinates are filtered to ensure unique coor-
 203 dinate pairs. Next, coordinates are filtered to decrease point density and speed the next
 204 step of fitting a third-degree piecewise affine spline to the filtered coordinates. The spline
 205 is parameterized using the sonar record’s unique id and the time elapsed. Finally, new
 206 coordinates are then predicted for each sonar record using the spline, resulting in sonar
 207 records with unique coordinate pairs along the smoothed vessel course spaced assum-
 208 ing a constant speed. These steps further improve rectification of sonograms along sin-
 209 uous river reaches.

210 2.6 Processing Large Recordings

211 The duration of a sonar survey and the range setting dictate the size of the sonar
 212 recording file, which can become prohibitively large for a typical computer to process.
 213 Therefore, PING-Mapper was designed to process sonar recordings in chunks. The chunk
 214 size sets the number of ping returns that will be read into memory for each sonar beam.
 215 A value of 500 is found to be appropriate in most scans but can be altered by users based
 216 on available computing resources. This any modern computer to process sonar record-
 217 ings of any size.

218 Another advantage to processing sonar recordings in chunks is that multiple chunks
 219 can be processed concurrently. PING-Mapper supports multi-threaded processing to ex-
 220 tract ping attributes, export non-rectified imagery, and sonogram georectification and
 221 export, resulting in decreasing overall processing time. Tests were conducted on a 01h:00m:06s
 222 sonar recording to determine speed of processing and data export. PING-Mapper is able
 223 to process and export all possible data products in 00h:41m:14s on a typical computer.
 224 Assuming a typical day in the field can result in upwards of 8h of sonar recordings, PING-
 225 Mapper could be set to process the data over night with datasets ready for analysis the
 226 next morning. Additional information is provided in Supplement Information Section
 227 Computational Performance and Table 2.

228 3 Case Studies

229 The following three case studies illustrate some analyses that can be undertaken
 230 with outputs from PING-Mapper. First, WCP sonar mosaics are used to locate and map

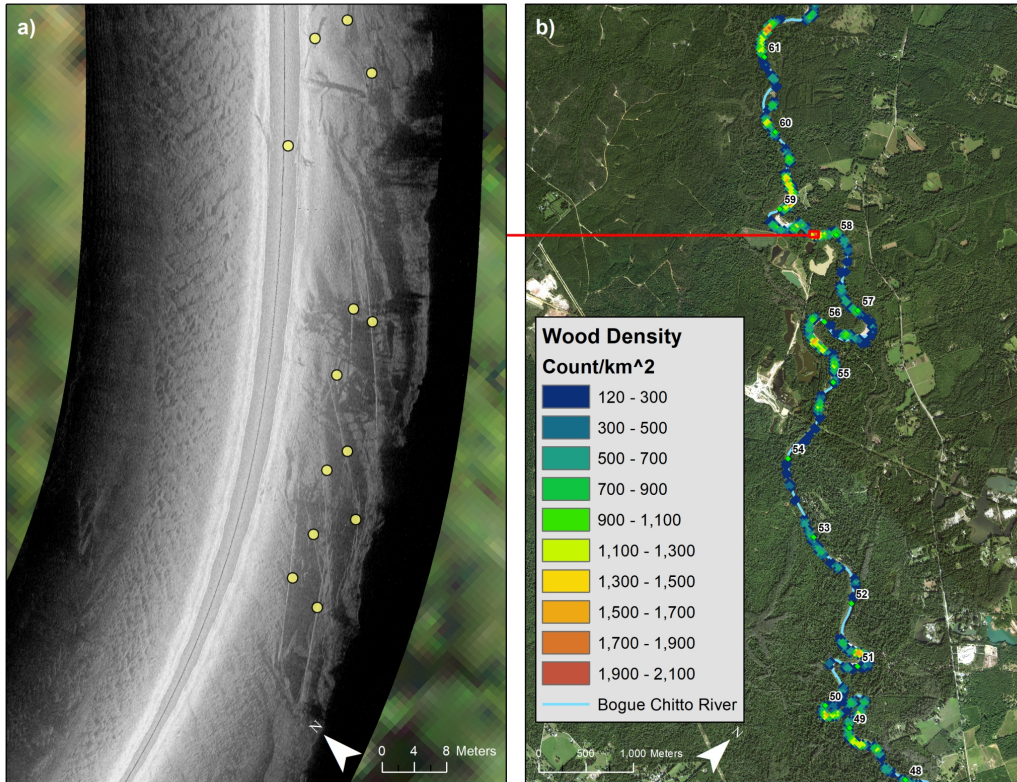


Figure 2. Example of locating and mapping large woody debris in the Bogue Chitto River in Mississippi. Panel (a) shows a georectified sonogram with water column present, with yellow points indicating location of large woody debris. Panel (b) shows wood density count per square kilometer.

231 large woody debris distribution in the Bogue Chitto River, MS. Second, sonar depth estimates from two survey transects on the Pearl River, MS allow creation longitudinal depth profiles and basic bathymetric surfaces. Finally, WCR sonar mosaics are visually interpreted to identify and delineate substrates on the Leaf River, MS. All sonar data were collected with a Humminbird Solix Chirp Mega SI+ sonar instrument operating at a nominal central frequency of 1.2 MHz with unknown frequency bandwidth; however, similar results are expected from any modern Humminbird model.

238 3.1 Mapping Large Woody Debris

239 Large woody debris present in aquatic environments serve important ecological functions for various species (Dolloff & Warren, 2003). Surveying rivers with SSS has proven successful in locating large-woody debris (Holcomb et al., 2020; Kaeser & Litts, 2008). SSS data were collected on the Bogue Chitto River, MS approximately 54 to 63 river kilometers (RKM) upstream of the confluence with the Pearl River on March 2, 2021. The sonar data were post-processed using PING-Mapper and georectified sonograms with the water column present were exported. Large woody debris were visually identified in a GIS by their distinguishing characteristic of long, linear edges and the shadows that they cast. Points were then placed on identified wood throughout the survey reach (Figure 2a). Finally, mapping the density of these points illustrates variation in wood presence across river reaches (Figure 2b).

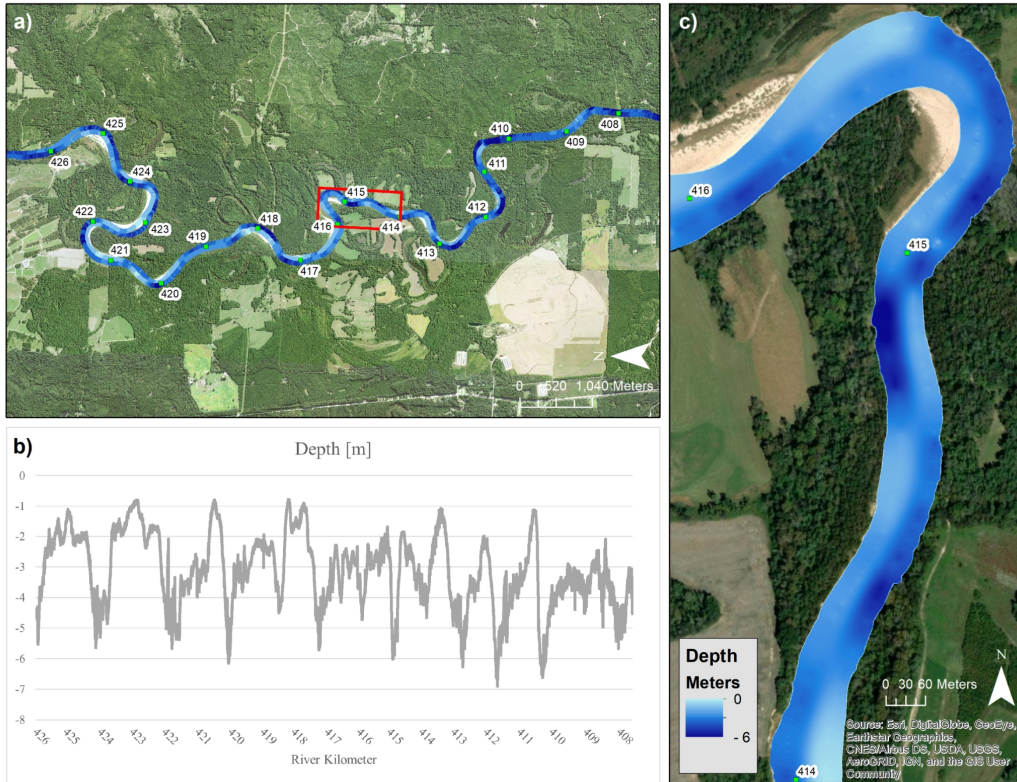


Figure 3. Example of mapping depth with SSS. Panel (a) shows sonar depths from two adjacent survey transects across 18 river kilometers on the Pearl River in Mississippi, surveyed upstream (RKM 426) to downstream (RKM 408). Panel (b) shows depth readings from the transect on the right side of the channel. Panel (c) shows an interpolated surface derived from the two transects and constrained by manually digitized banklines. To digitize the banklines, WCR georectified mosaics were exported and brought into a GIS where they were visually interpreted to determine the location of the bank, and a polyline was digitized along the bank.

3.2 Mapping Bathymetry

Two SSS survey transects from two vessels spaced to reduce interference were conducted on the Pearl River, MS on March 4, 2021, from RKM 426 to 408. One vessel surveyed the left side of the channel and the other right, moving upstream to downstream. Sonar depth estimates from down-facing beams are shown for two transects (Figure 3a) and a longitudinal profile for the river-right transect (Figure 3b) shows that our software is able to position and map the sonar data to capture the complex bathymetry in the sequence of riffles and pools. The sonogram mosaics and satellite imagery were used to delineate channel bank lines in a geographic information system (GIS). The bank lines constrained an inverse distance weighting (IDW) interpolation of the two transects to generate a bathymetric surface (Figure 3c).

3.3 Mapping Substrate

Scanning a waterbody with SSS results in imagery with tones and textures that can be associated with different types of substrate (Kaesler & Litts, 2010). Once georectified, the sonograms are brought into a GIS for visual interpretation and manual delin-

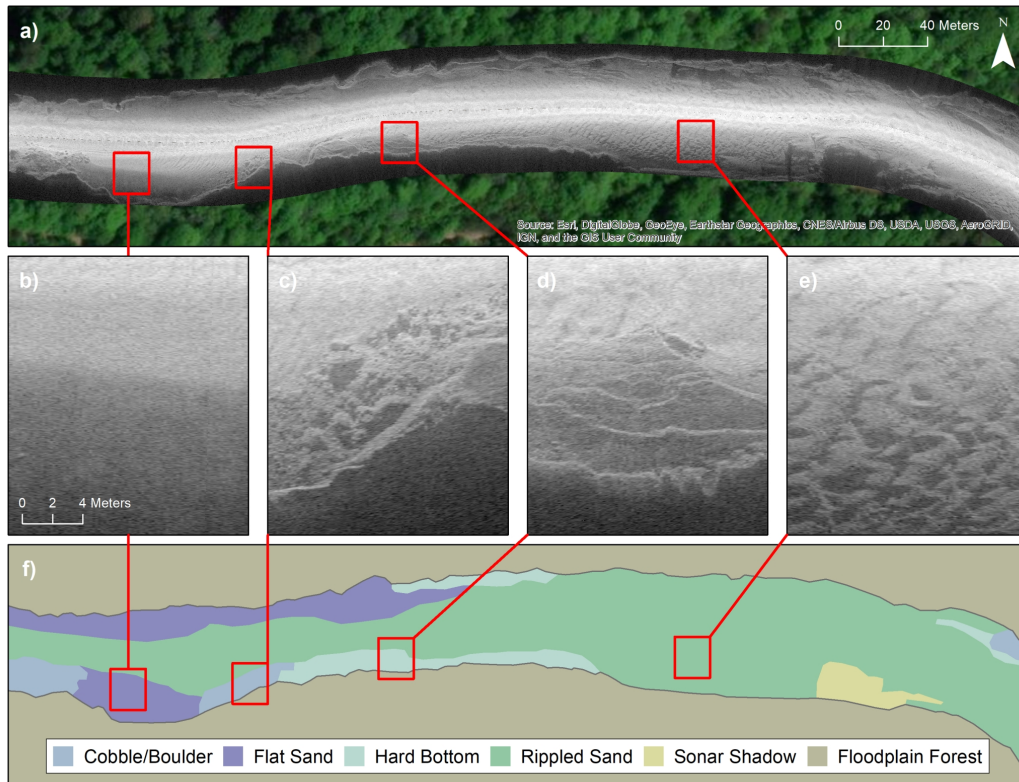


Figure 4. Example of delineating and classifying substrate on the Leaf River, MS. Panel (a) shows georectified sonograms with the water column removed. Detail views of the sonograms show (b) flat sand; (c) cobble/boulder; (d) hard bottom; and (e) rippled sand. Panel (f) shows a map of the substrate boundaries visually identified and manually delineated in a GIS.

265 eation of polygons, resulting in maps showing coverage and distribution of substrates at
 266 large spatial extents. The Leaf River, MS, was scanned 138 RKM upstream of the Pascagoula
 267 River confluence on May 6, 2021. The sonar recordings were processed with PING-Mapper
 268 and georectified sonograms with the water column removed were exported (4a). Differ-
 269 ent substrate types were visually identified and polygons were manually digitized in a
 270 GIS to delineate substrate boundaries. Smooth, homogeneous textures are associated
 271 with flat sand bedforms (4b); blocky textures with shadows are associated with boulder
 272 and cobble (4c); sharp edges indicating terracing are associated with hard bottom
 273 (4d); and wavy, chevron textures with shadows are associated with rippled sand (4e).
 274 Portions of the sonogram with the same substrate characteristics were delineated with
 275 a polygon, resulting in a map of substrate distribution (4f).

276 4 Discussion

277 PING-Mapper is a new Python toolbox for decoding and exporting benthic datasets
 278 from Humminbird SSS instruments. It builds and improves upon previous algorithms
 279 (Buscombe, 2017) for depth detection and georectification, and speeds processing and
 280 export. The software is designed to 1) decode sonar recordings from any Humminbird
 281 system; 2) export ping attributes from every sonar channel; 3) use sonar sensor depth
 282 or automated depth detection for water column removal; and 4) exports sonogram tiles

283 and georectified mosaics. The software are hosted in a public repository to ensure equ-
 284 itable access.

285 Aquatic scientists are increasingly using SSS to inform a range of research efforts.
 286 This includes mapping essential habitats (Kaeser & Litts, 2008; Cheek et al., 2016; Walker
 287 & Alford, 2016; Holcomb et al., 2020), informing invasive species competition for discrete
 288 habitat patches (Gocłowski et al., 2013; Prechtel et al., 2018), enhancing habitat mod-
 289 eling for aquatic species (Smit & Kaeser, 2016; Kaeser et al., 2019), and mapping aquatic
 290 vegetation (Gumusay et al., 2019). Studies like these depend on the ability to easily con-
 291 vert output from recreation-grade sonar systems into reproducible datasets with min-
 292 imal expertise in data processing. PING-Mapper provides a suite of algorithms to fa-
 293 cilitate this conversion. More importantly, these tools generate large datasets quickly which
 294 allow scientific studies to be conducted at increasing spatial and temporal scales rele-
 295 vant to numerous disciplines in ecological, environmental, and physical sciences concerned
 296 with the form and character of benthic environments and the life they support.

297 The creation of a recreation-grade sonar processing pipelines allows opportunities
 298 for future research, analysis, and applications of datasets generated by PING-Mapper.
 299 For example, a primary use of side scan sonar image mosaics is to locate and map sub-
 300 strate distributions throughout aquatic systems. Visual identification and manual dig-
 301 itization is common practice (Kaeser et al., 2013) but automated machine learning ap-
 302 proaches such as Buscombe and Goldstein (2022) show promise. Future work will focus
 303 on developing and integrating automated substrate segmentation and classification work-
 304 flows to inform landscape-level aquatic studies. Reliable depth measurements are nec-
 305 essary to ensure accurate spatial positioning and coverage of automated substrate maps
 306 generated from sonogram mosaics, therefore automated depth detection routines such
 307 as Zheng et al. (2021) will be incorporated in the future. Potential improvements for the
 308 marine environment include implementing attitude adjustment (i.e., pitch, yaw and roll)
 309 and incorporating salinity to better locate the bed (Blondel, 2009).

310 The goal of this software is to address the growing and evolving data processing
 311 needs of the aquatic research community by including recreation-grade sonar datasets
 312 in their research. Particular emphasis has been placed on making PING-Mapper an open
 313 source tool for benthic applications and research. The code is designed to be modular
 314 and object oriented to facilitate contributions, modifications, and new applications from
 315 the community. This software is the first of its kind in that it allows any engaged cit-
 316 izen or researcher working in any aquatic waterbody to image their system with zero soft-
 317 ware costs and full reproducibility.

318 **Data Availability Statement**

319 The code for PING-Mapper and test sonar recordings are available on Zenodo and
 320 GitHub via Bodine and Buscombe (2022).

321 **Acknowledgments**

322 This study was made possible by a partnership between the U.S. Fish and Wildlife
 323 Service and Northern Arizona University. Funding for this work was provided by the Open
 324 Ocean Restoration Area Trustee Implementation Group of the Deepwater Horizon Trustee
 325 Council as part of their Final Restoration Plan 1 for birds and sturgeon. The findings
 326 and conclusions in this article are those of the authors and do not necessarily represent
 327 the views of the U.S. Fish and Wildlife Service. Thanks to Channing St. Aubin (USFWS),
 328 Mike Andres (USM), Eric Haffey (USM), Kasea Price (USM), and Katherine Wright (USM)
 329 for data collection and planning, and to Daniel Haught (USGS) for testing.

330 Supporting Information

331 Computational Performance

332 The software is designed to speed processing and dataset export through multi-threaded
 333 processing. Export of plots, tiles and rectified sonograms account for the largest propor-
 334 tion of the total processing time, therefore running these algorithms in parallel result in
 335 significant decrease in total processing time. Algorithms which were parallelized include
 336 decoding and export of SON ping metadata, export of bedpick plots, export of sonogram
 337 tiles, and export of rectified sonogram GeoTiffs. Portions of the software that run se-
 338 quentially (e.g., non-parallelized) include decode and export of DAT metadata, deter-
 339 mining SON file structure, depth processing, trackline smoothing, and mosaic rectified
 340 sonograms.

341 The computational performance of PING-Mapper was tested with a sonar record-
 342 ing from a Humminbird Helix with Mega imaging. Sonar recording includes high-frequency
 343 down image (200 kHz), very high-frequency down image (1.2 MHz), and two very high-
 344 frequency side scan images (1.2 MHz). Total duration of the recording is 01:00:06 (hh:mm:ss).
 345 Total ping count is 279,916. Range setting is 1,398 returns per ping, or 26.6m. Chunk
 346 size is set to 512 pings, resulting in the following exports: 547 WCP sonograms; 274 WCR
 347 sonograms; 137 bedpick plots; 274 WCP rectified GeoTiffs; 274 WCR rectified GeoTiffs;
 348 and mosaics for WCP and WCR.

349 Tests were run on a Windows 10 laptop with Intel i7-8650U 1.90 GHz CPU, 16 GB
 350 of memory, and 500 GB solid state hard drive. Each test was run with an increasing num-
 351 ber of processing threads (t), including $t = 1, 2, 4, 6,$ and 8 threads. All other param-
 352 eters remained the same. Processing time, in seconds, are shown for the main compo-
 353 nents of the software in Table 2. Total processing time is reported in seconds as well as
 354 hours, minutes, and seconds (hh:mm:ss) for reference. Sequential algorithm processing
 355 time remained approximately constant with varying number of process threads. The al-
 356 gorithm for decoding SON scales with number of threads until the number of threads
 357 is equal to the number of beams, then remains roughly constant for $t > 4$. The algo-
 358 rithms to export bedpick plots, sonogram tiles, and rectify sonograms had decreasing pro-
 359 cessing time with increasing t .

Table 1. Humminbird SON file structure for specified sonar models: 9xx series, 11xx series, Helix, Onyx, and Solix. Other models presumably follow a similar pattern. The Name and Description indicate the type of data available for each ping in a Humminbird sonar recording. The Hex Tag is the 8-bit hexadecimal value preceding the data value. For each of the Humminbird models, the offset from the beginning of the recording is given for the respective data type. This pattern repeats for each ping for the duration of the sonar recording.

Name	Description	Hex Tag	Data Offset (by model)		
			9xx	11xx; Helix; Onyx	Solix
Ping #1	Beginning of ping #1	C0	+0	+0	+0
Header Start	Beginning of ping header	21	+3	+3	+3
Record Number	Unique ping ID	80	+5	+5	+5
Time Elapsed	Time elapsed (msec)	81	+10	+10	+10
UTM X	EPSG 3395 easting coord.	82	+15	+15	+15
UTM Y	EPSG 3395 northing coord.	83	+20	+20	+20
Heading Quality	Quality flag ¹	84	+25	+25	+25
Heading	Heading (1/10 deg)	-	+27	+27	+27
Speed Quality	Quality flag ¹	85	+30	+30	+30
Speed	Vessel speed (cm/sec)	-	+32	+32	+32
NA	Unknown data contents	86	-	+35	+35
Depth	Sonar depth (cm)	87	+35	+40	+40
NA	Unknown data contents	-	-	-	+44-83
Sonar Beam	Sonar beam ID ²	50	+40	+45	+85
Voltage	Voltage scale (1/10 volt)	51	+42	+47	+87
Frequency	Sonar beam frequency (Hz)	92	+44	+49	+89
NA	Unknown data contents	-	+48-60	+53-65	+89-145
Return Count	Number ping returns (n)	A0	+62	+67	+147
Header End	End of ping header	21	+66	+72	+152
Ping Returns	Sonar intensity [0-255]	21	+67	+73	+153
Ping #2	Beginning of ping #2	21	+67+ n +1	+73+ n +1	+152+ n +1
... ³

¹ 0=bad; 1=good.

² 0=Down Scan Low Freq.; 1=Down Scan Hi Freq.; 2=Side Scan Port-side; 3=Side Scan Starboard;
4=Down Scan Megahertz.

³ Pattern repeats for duration of sonar recording.

Table 2. Computation time for sequential and multi-threaded algorithms on a test dataset^c.

Threads (<i>t</i>)	Sequential Algorithms ^b	Decode SON ^c	Bedpick Plots ^c	Sonogram Tiles ^c	Rectify Sonograms ^c	Total (s)	Total (hh:mm:ss)
1	367.3	52.8	423.3	1158.6	4349.0	6351.0	01:45:51
2	363.4	35.3	261.0	723.2	3197.1	4580.0	01:16:20
4	361.5	25.7	186.7	531.2	1960.9	3066.0	00:51:06
6	359.0	23.9	179.6	533.7	1451.8	2548.0	00:42:28
8	363.2	24.0	175.8	522.1	1388.9	2474.0	00:41:14

^a Test dataset from a Humminbird Helix with Mega imaging. Sonar recording includes high-frequency down image (200 kHz), very high-frequency down image (1.2 MHz), and two very high-frequency side scan images (1.2 MHz). Total duration of the recording is 01:00:06 (hh:mm:ss). Total ping count is 279,915. Range setting is 1,398 returns per ping, or 26.6m.

^b Sequential (e.g., non-parallel) algorithms include decoding DAT file, determining SON file structure, depth processing, trackline smoothing, and generating rectified mosaics.

^c Multi-threaded processing algorithm.

References

- 360
- 361 Andreadis, K. M., Schumann, G. J. P., & Pavelsky, T. (2013). A simple global river
362 bankfull width and depth database. *Water Resources Research*, *49*(10), 7164–
363 7168. doi: <https://doi.org/10.1002/wrcr.20440>
- 364 Barnosky, A. D., Matzke, N., Tomiya, S., Wogan, G. O. U., Swartz, B., Quental,
365 T. B., ... Ferrer, E. A. (2011). Has the Earth’s sixth mass extinction already
366 arrived? *Nature*. doi: <https://doi.org/10.1038/nature09678>
- 367 Biggs, J., von Fumetti, S., & Kelly-Quinn, M. (2017). The importance of small
368 waterbodies for biodiversity and ecosystem services: implications for policy
369 makers. *Hydrobiologia*, *793*(1), 3–39. doi: [10.1007/s10750-016-3007-0](https://doi.org/10.1007/s10750-016-3007-0)
- 370 Blondel, P. (2009). *The Handbook of Sidescan Sonar*. Berlin, Heidelberg: Springer
371 Berlin Heidelberg. doi: <https://doi.org/10.1007/978-3-540-49886-5>
- 372 Bock, M., Xofis, P., Mitchley, J., Rossner, G., & Wissen, M. (2005). Object-oriented
373 methods for habitat mapping at multiple scales – Case studies from Northern
374 Germany and Wye Downs, UK. *Journal for Nature Conservation*, *13*(2-3),
375 75–89. doi: <https://doi.org/10.1016/j.jnc.2004.12.002>
- 376 Bodine, C. S., & Buscombe, D. (2022). *PING-Mapper [Computer Software]*. doi:
377 <https://doi.org/10.5281/zenodo.6604785>
- 378 Brown, C. J., Smith, S. J., Lawton, P., & Anderson, J. T. (2011). Benthic habitat
379 mapping: A review of progress towards improved understanding of the spatial
380 ecology of the seafloor using acoustic techniques. *Estuarine, Coastal and Shelf
381 Science*, *92*(3), 502–520. doi: <https://doi.org/10.1016/j.ecss.2011.02.007>
- 382 Buscombe, D. (2017). Shallow water benthic imaging and substrate characteri-
383 zation using recreational-grade sidescan-sonar. *Environmental Modelling and
384 Software*, *89*, 1–18. doi: <https://doi.org/10.1016/j.envsoft.2016.12.003>
- 385 Buscombe, D., & Goldstein, E. B. (2022). A Reproducible Pipeline for Geoscientific
386 Image Segmentation with Fully Convolutional Models. *Earth and Space Sci-
387 ence*.
- 388 Buscombe, D., Grams, P. E., & Smith, S. M. C. (2016). Automated Riverbed
389 Sediment Classification Using Low-Cost Sidescan Sonar. *Journal of Hy-
390 draulic Engineering*, *142*(2), 6015019. doi: [https://doi.org/10.1061/
391 \(ASCE\)HY.1943-7900.0001079](https://doi.org/10.1061/(ASCE)HY.1943-7900.0001079)
- 392 Cael, B. B., Heathcote, A. J., & Seekell, D. A. (2017). The volume and mean depth
393 of Earth’s lakes. *Geophysical Research Letters*, *44*(1), 209–218. doi: [https://
394 doi.org/10.1002/2016GL071378](https://doi.org/10.1002/2016GL071378)
- 395 Cheek, B. D., Grabowski, T. B., Bean, P. T., Groeschel, J. R., & Magnelia, S. J.
396 (2016). Evaluating habitat associations of a fish assemblage at multiple spa-
397 tial scales in a minimally disturbed stream using low-cost remote sensing.
398 *Aquatic Conservation: Marine and Freshwater Ecosystems*, *26*(1), 20–34. doi:
399 [10.1002/aqc.2569](https://doi.org/10.1002/aqc.2569)
- 400 Chesterman, W. D., Clynick, P. R., & Stride, A. H. (1958). An acoustic aid to sea
401 bed survey. *Acta Acustica united with Acustica*, *8*(5).
- 402 Cobra, D. T., Oppenheim, A. V., & Jaffe, J. S. (1992). Geometric Distor-
403 tions in Side-Scan Sonar Images: A Procedure for Their Estimation and
404 Correction. *IEEE Journal of Oceanic Engineering*, *17*(3), 252–268. doi:
405 <https://doi.org/10.1109/48.153442>
- 406 Danovaro, R., Company, J. B., Corinaldesi, C., D’Onghia, G., Galil, B., Gambi, C.,
407 ... Tselepides, A. (2010). Deep-Sea Biodiversity in the Mediterranean Sea:
408 The Known, the Unknown, and the Unknowable. *PLOS ONE*, *5*(8), e11832.
409 doi: <https://doi.org/10.1371/JOURNAL.PONE.0011832>
- 410 Dolloff, C. A., & Warren, M. L., Jr. (2003). Fish Relationships with Large Wood
411 in Small Streams. In S. V. Gregory, K. L. Boyer, & A. M. Gurnell (Eds.), *The
412 ecology and management of wood in world rivers* (Vol. 37, pp. 179–193). Amer-
413 ican Fisheries Society. doi: <https://doi.org/10.47886/9781888569568.ch9>

- 414 Flowers, H. J., & Hightower, J. E. (2013). A Novel Approach to Surveying Stur-
 415 geon Using Side-Scan Sonar and Occupancy Modeling. *Marine and Coastal*
 416 *Fisheries*, 5(1), 211–223. doi: 10.1080/19425120.2013.816396
- 417 Fu, H., Zhong, J., Yuan, G., Ni, L., Xie, P., & Cao, T. (2014). Functional traits
 418 composition predict macrophytes community productivity along a water depth
 419 gradient in a freshwater lake. *Ecology and Evolution*, 4(9), 1516–1523. doi:
 420 10.1002/ece3.1022
- 421 Gocłowski, M. R., Kaeser, A. J., & Sammons, S. M. (2013). Movement and Habi-
 422 tat Differentiation among Adult Shoal Bass, Largemouth Bass, and Spotted
 423 Bass in the Upper Flint River, Georgia. *North American Journal of Fisheries*
 424 *Management*, 33(1), 56–70. doi: 10.1080/02755947.2012.741555
- 425 Gumusay, M. U., Bakirman, T., Tuney Kizilkaya, I., & Aykut, N. O. (2019). A
 426 review of seagrass detection, mapping and monitoring applications using
 427 acoustic systems. *European Journal of Remote Sensing*, 52(1), 1–29. doi:
 428 10.1080/22797254.2018.1544838
- 429 Holcomb, K. M., Schueller, P., Jelks, H. L., Knight, J. R., & Allen, M. S. (2020).
 430 Use of Strong Habitat–Abundance Relationships in Assessing Popula-
 431 tion Status of Cryptic Fishes: An Example Using the Harlequin Darter.
 432 *Transactions of the American Fisheries Society*, 149(3), 320–334. doi:
 433 <https://doi.org/10.1002/tafs.10231>
- 434 Johansen, M. (2013). *HumViewer (Version 86) [Computer Software]*. Retrieved from
 435 <https://humviewer.cm-johansen.dk/>
- 436 Kaeser, A. J., & Litts, T. L. (2008). An Assessment of Deadhead Logs and Large
 437 Woody Debris Using Side Scan Sonar and Field Surveys in Streams of South-
 438 west Georgia. *Fisheries*, 33(12), 589–597. doi: [https://doi.org/10.1577/](https://doi.org/10.1577/1548-8446-33.12.589)
 439 [1548-8446-33.12.589](https://doi.org/10.1577/1548-8446-33.12.589)
- 440 Kaeser, A. J., & Litts, T. L. (2010). A Novel Technique for Mapping Habitat in
 441 Navigable Streams Using Low-cost Side Scan Sonar. *Fisheries*, 35(4), 163–174.
 442 doi: <https://doi.org/10.1577/1548-8446-35.4.163>
- 443 Kaeser, A. J., Litts, T. L., & Tracy, T. W. (2013). Using low-cost side-scan sonar
 444 for benthic mapping throughout the lower Flint River, Georgia, USA. *River*
 445 *Research and Applications*, 29(5), 634–644. doi: [https://doi.org/10.1002/](https://doi.org/10.1002/rra.2556)
 446 [rra.2556](https://doi.org/10.1002/rra.2556)
- 447 Kaeser, A. J., Smit, R., & Gangloff, M. (2019). *Mapping and modeling the distri-*
 448 *bution, abundance, and habitat associations of the endangered fat threeridge in*
 449 *the Apalachicola river system* (Vol. 10) (No. 2). U.S. Fish and Wildlife Service.
 450 doi: 10.3996/032019-JFWM-021
- 451 Kerr, J. T., & Ostrovsky, M. (2003). From space to species: ecological applica-
 452 tions for remote sensing. *Trends in Ecology & Evolution*, 18(6), 299–305. doi:
 453 [https://doi.org/10.1016/S0169-5347\(03\)00071-5](https://doi.org/10.1016/S0169-5347(03)00071-5)
- 454 Klein, M., & Edgerton, H. (1968). Sonar a modern technique for ocean exploita-
 455 tion. *IEEE Spectrum*, 5(6), 40–46. doi: [https://doi.org/10.1109/MSPEC.1968](https://doi.org/10.1109/MSPEC.1968.5214684)
 456 [.5214684](https://doi.org/10.1109/MSPEC.1968.5214684)
- 457 Leraand Engineering Inc. (2022). *SonarTRX [Computer Software]*. Retrieved from
 458 <https://www.sonartrx.com/>
- 459 Longhurst, A. R. (2007). *Ecological Geography of the Sea* (Second ed.). Elsevier Inc.
 460 doi: <https://doi.org/10.1016/B978-0-12-455521-1.X5000-1>
- 461 Murphy, K. J. (2021). Open-Source Science: The NASA Earth Science Perspective.
 462 *The Earth Observer*. Retrieved from [https://earthdata.nasa.gov/learn/](https://earthdata.nasa.gov/learn/articles/open-source-science-nasa-earth-science-perspective)
 463 [articles/open-source-science-nasa-earth-science-perspective](https://earthdata.nasa.gov/learn/articles/open-source-science-nasa-earth-science-perspective)
- 464 Musale, A. S., & Desai, D. V. (2010). Distribution and abundance of macroben-
 465 thic polychaetes along the South Indian coast. *Environmental Monitoring and*
 466 *Assessment* 2010 178:1, 178(1), 423–436. doi: [https://doi.org/10.1007/S10661](https://doi.org/10.1007/S10661-010-1701-3)
 467 [-010-1701-3](https://doi.org/10.1007/S10661-010-1701-3)
- 468 Myrvold, K. M., & Dervo, B. K. (2020). Flight elevation and water clarity affect

- 469 the utility of unmanned aerial vehicles in mapping stream substratum. *Fish-*
 470 *eries Management and Ecology*, *27*(2), 167–169. doi: [https://doi.org/10.1111/](https://doi.org/10.1111/fme.12394)
 471 [fme.12394](https://doi.org/10.1111/fme.12394)
- 472 Parnum, I. M., Ellement, T., Perry, M. A., Parsons, M. J., & Tecchiato, S. (2017).
 473 Using recreational echo-sounders for marine science studies. In *Proceedings of*
 474 *ACOUSTICS 2017*. Retrieved from [http://cmst.curtin.edu.au/products/](http://cmst.curtin.edu.au/products/humconverter-software/)
 475 [humconverter-software/](http://cmst.curtin.edu.au/products/humconverter-software/)
- 476 Prechtel, A. R., Coulter, A. A., Etchison, L., Jackson, P. R., & Goforth, R. R.
 477 (2018). Range estimates and habitat use of invasive Silver Carp (*Hypoph-*
 478 *thalmichthys molitrix*): evidence of sedentary and mobile individuals. *Hydrobi-*
 479 *ologia*, *805*(1), 203–218. doi: [10.1007/s10750-017-3296-y](https://doi.org/10.1007/s10750-017-3296-y)
- 480 ReefMaster Software Ltd. (2021). *ReefMaster [Computer Software]*. Retrieved from
 481 <https://reefmaster.com.au/>
- 482 Sánchez-Carnero, N., Rodríguez-Pérez, D., Couñago, E., Aceña, S., & Freire,
 483 J. (2012). Using vertical Sidescan Sonar as a tool for seagrass cartogra-
 484 phy. *Estuarine, Coastal and Shelf Science*, *115*, 334–344. doi: [10.1016/](https://doi.org/10.1016/j.ecss.2012.09.015)
 485 [j.ecss.2012.09.015](https://doi.org/10.1016/j.ecss.2012.09.015)
- 486 Schmidt, B. A., Tucker, T. R., Collier, J. J., Mayer, C. M., Roseman, E. F., Stott,
 487 W., & Pritt, J. J. (2020). Determining habitat limitations of Maumee River
 488 walleye production to western Lake Erie fish stocks: documenting a spawn-
 489 ing ground barrier. *Journal of Great Lakes Research*, *46*(6), 1661–1673. doi:
 490 <https://doi.org/10.1016/j.jglr.2020.08.022>
- 491 Scholl, E. A., Cross, W. F., Baxter, C. V., & Guy, C. S. (2021). Uncovering pro-
 492 cess domains in large rivers: Patterns and potential drivers of benthic sub-
 493 strate heterogeneity in two North American riverscapes. *Geomorphology*, *375*,
 494 107524. doi: <https://doi.org/10.1016/j.geomorph.2020.107524>
- 495 Singh, H., Adams, J., Mindell, D., & Foley, B. (2000). Imaging underwater for ar-
 496 chaeology. *International Journal of Phytoremediation*, *21*(1), 319–328. doi:
 497 <https://doi.org/10.1179/jfa.2000.27.3.319>
- 498 Smit, R., & Kaeser, A. J. (2016). Defining freshwater mussel mesohabitat associa-
 499 tions in an alluvial, Coastal Plain river. *Freshwater Science*, *35*(4), 1276–1290.
 500 doi: [10.1086/688928](https://doi.org/10.1086/688928)
- 501 Smith, K. F., & Brown, J. H. (2002). Patterns of Diversity, Depth Range and
 502 Body Size among Pelagic Fishes along a Gradient of Depth. *Global Ecol-*
 503 *ogy and Biogeography*, *11*(4), 313–322. doi: [https://doi.org/10.1046/](https://doi.org/10.1046/j.1466-822X.2002.00286.x)
 504 [j.1466-822X.2002.00286.x](https://doi.org/10.1046/j.1466-822X.2002.00286.x)
- 505 Tickner, D., Opperman, J. J., Abell, R., Acreman, M., Arthington, A. H., Bunn,
 506 S. E., . . . Young, L. (2020). Bending the Curve of Global Freshwater Biodi-
 507 versity Loss: An Emergency Recovery Plan. *BioScience*, *70*(4), 330–342. doi:
 508 <https://doi.org/10.1093/BIOSCI/BIAA002>
- 509 Walker, D. J., & Alford, J. B. (2016). Mapping Lake Sturgeon Spawning Habitat
 510 in the Upper Tennessee River using Side-Scan Sonar. *North American Jour-*
 511 *nal of Fisheries Management*, *36*(5), 1097–1105. doi: [10.1080/02755947.2016](https://doi.org/10.1080/02755947.2016.1198289)
 512 [.1198289](https://doi.org/10.1080/02755947.2016.1198289)
- 513 Weiers, S., Bock, M., Wissen, M., & Rossner, G. (2004). Mapping and indicator
 514 approaches for the assessment of habitats at different scales using remote sens-
 515 ing and GIS methods. *Landscape and Urban Planning*, *67*(1-4), 43–65. doi:
 516 [https://doi.org/10.1016/S0169-2046\(03\)00028-8](https://doi.org/10.1016/S0169-2046(03)00028-8)
- 517 Yan, J., Meng, J., & Zhao, J. (2021). Bottom detection from backscatter data of
 518 conventional side scan sonars through 1d-unet. *Remote Sensing*, *13*(5). doi:
 519 <https://doi.org/10.3390/rs13051024>
- 520 Yang, J., Gong, P., Fu, R., Zhang, M., Chen, J., Liang, S., . . . Dickinson, R. (2013).
 521 The role of satellite remote sensing in climate change studies. *Nature Climate*
 522 *Change*, *3*(10), 875–883. doi: <https://doi.org/10.1038/nclimate1908>
- 523 Zhao, W., Hu, A., Ni, Z., Wang, Q., Zhang, E., Yang, X., . . . Wang, J. (2019). Bio-

524 diversity patterns across taxonomic groups along a lake water-depth gradient:
525 Effects of abiotic and biotic drivers. *Science of The Total Environment*, 686,
526 1262–1271. doi: 10.1016/j.scitotenv.2019.05.381
527 Zheng, G., Zhang, H., Li, Y., & Zhao, J. (2021). A Universal Automatic Bottom
528 Tracking Method of Side Scan Sonar Data Based on Semantic Segmentation.
529 *Remote Sensing*, 13(10), 1945. Retrieved from [https://www.mdpi.com/](https://www.mdpi.com/2072-4292/13/10/1945)
530 2072-4292/13/10/1945 doi: <https://doi.org/10.3390/rs13101945>